

## Yield Stress Development during Age-Hardening of AA6xxx: Comparison of Two Model Predictions with Experimental Findings

Thiemo Brüggemann<sup>1</sup>, Christian Bollmann<sup>1</sup>, Volker Mohles<sup>1</sup>, Günter Gottstein<sup>1</sup>, Jürgen Hirsch<sup>2</sup>, and Ole Runar Myhr<sup>3</sup>

<sup>1</sup>Institute of Physical Metallurgy and Metal Physics, RWTH-Aachen University, Kopernikusstrasse 14, D-52056 Aachen, Germany

<sup>2</sup>Hydro Aluminium Deutschland GmbH, Research and Development, Georg-von-Boeselager-Strasse 25, 53117 Bonn, Germany

<sup>3</sup>Hydro Automotive Structures, N-2831, Raufoss, Norway

The yield stress development of various Al-Mg-Si alloys was modeled by two work hardening simulation tools and compared to experimental results. Four different alloys were used: Three high-purity ternary laboratory alloys, i.e. Al-0.4wt%Mg-0.4wt%Si, Al-0.6wt%Mg-0.8wt%Si, and Al-0.4wt%Mg-1.0wt%Si; plus a commercial AA6016 alloy with 0.45wt%Mg-1.0wt%Si besides further elements. The age-hardening-behavior during artificial ageing was recorded via hardness and tensile testing. Yield stress modeling was performed with two simulation tools: *3IVM+*, developed at IMM RWTH-Aachen University, a dislocation density based work hardening model assuming a cellular dislocation structure; and *NaMo*, developed by O. R. Myhr and Ø. Grong, a yield stress model adding various strength contributions to obtain the overall yield stress. To be able to simulate the observed yield stress development, knowledge on the actual microchemistry is essential. NaMo contains a built-in microchemistry model. For *3IVM+* these data needed to be extracted from assumptions and experimental findings. The comparison of experimental results to model predictions will be discussed.

**Keywords:** Al-Mg-Si, age hardening, yield-stress modeling, evolution of precipitates.

### 1. Introduction

For car body applications heat-treatable aluminum alloys compete with steel. The main properties which are needed for such applications are formability and a high strength to weight ratio. While good formability is wanted during metal forming of car body sheets, high strength is desired for the final condition.

Due to the fact that the microstructure defines the mechanical properties of a metal product, the change of microstructure during thermo-mechanical processing needs to be understood in order to improve the quality of the manufactured good. Aluminum alloys which are widely used for such applications are heat treatable Al-Mg-Si alloys. They are produced along the standard process chain for aluminum alloys. To obtain both maximum age hardening response and good formability, the material is solution heat treated, followed by rapid quenching to retain the alloying elements in solid solution. Having a low strength but high formability at this stage, the material is then delivered to the customer, where it is processed to car body parts via metal forming. The final in-service strength is then achieved through age-hardening in an artificial ageing paint-bake cycle, where the material is heated at about 180 °C for several minutes.

To ensure faster optimization of both process variables and alloys, simulation tools predicting the impact of material properties on the process and vice versa, have widely been accepted as research instruments [1, 2]. During age hardening the main variables influencing the final properties are connected to a change in microchemistry. Without a precise description of microchemistry no simulation of technically important material properties, such as yield stress, is possible. Hence, the

dramatic change of precipitate condition during age hardening of AA6xxx makes a microstructure model a crucial part of the whole simulation sequence [1, 3-4].

In this paper the evolution of yield stress of various high purity ternary Al-Mg-Si laboratory alloys in comparison to an industrial AA6016 alloy with ageing time during artificial ageing was simulated by two models: The dislocation density based flow stress model 3IVM+ [5-8], and the particle size distribution and strength model NaMo [1, 4]. Modeling of microchemistry evolution will be looked upon in detail. To extract necessary information for simulation and to validate modeling results, experimental data at different ageing times were recorded via hardness measurements, tensile tests and some TEM measurements.

## 2. Experimental Procedure

Four AA6xxx alloys were supplied by HYDRO Aluminium R & D, Bonn, i.e. three laboratory-alloys containing high purity aluminum (> 5 N) with different weight contents of Mg and Si added, and a commercial AA6016 alloy. Labeling and chemical compositions of the alloys are shown in Table 1.

Table 1: Chemical compositions of alloys used, in wt-%

	Mg	Si	Fe	Cu	Mn	Cr	Zn	Ti
Material 1	0.4	0.4	-	-	-	-	-	-
Material 2	0.6	0.8	-	-	-	-	-	-
Material 3	0.4	1.0	-	-	-	-	-	-
Material P [AA6016]	0.4477	1.0293	0.2804	0.0412	0.0644	0.0113	0.0106	0.0192

The laboratory alloys were delivered in an as-extruded condition with dimensions of 3 mm \* 20 mm \* 1000 mm. Material P was delivered in cold-rolled (sheet thickness = 1 mm), solution heat treated and naturally aged (14 days) condition. To bring the laboratory alloys into a comparable condition as material P, they were homogenized for 1 h at 560 °C, water quenched, and cold rolled from 3 mm to 1 mm.

For hardness measurements all materials were solution heat treated at 540 °C for 1 minute holding time, water quenched, and subsequently aged at 180 °C in a forced-circulation air furnace. In between treatments samples were stored in liquid nitrogen. After various ageing times the Vickers Hardness (HV 0.3) was measured; from each sample at least 5 indentations were taken.

Processing of tensile testing specimens was performed according to the same rolling/ heat treatment schedule as for hardness specimens. Samples were aged from ageing times  $t_{AA} = 0$  min up to the respective peak age time  $t_{PA}$ , which was determined from the HV observations. Every material and ageing time combination was measured with three tensile specimens to obtain good statistics.

## 3. Microchemistry Modeling

As already mentioned the change of microchemistry during precipitation plays an important role for the yield stress evolution during ageing. This is in particular valid for the used range of age hardenable alloys, where the strength of a peak-aged sample can be up to five times higher than a sample in solution heat treated condition, as shown in [5]. The main parameters which comprise the microchemistry are volume fraction of particles, particle size distribution and shape, particle coherency with matrix, number density of particles, solute content of alloying elements, and grain size. For the used ageing temperature of 180 °C the grain size was assumed to be constant.

Since the dislocation based hardening model 3IVM+ does not include a microchemistry model, the evolution of the above mentioned parameters over ongoing ageing time had to be derived from experimental findings and respective assumptions. First of all, the hardness evolution during ageing time  $t_{AA}$  was related to the increase of volume fraction of particles, which is suitable when assuming

that precipitation in Al-Mg-Si alloys is a nucleation and growth process [3]. Thus, the hardness-increase  $\Delta HV$  over ageing time  $t_{AA}$  at 180 °C of every material  $i$  was normalized by Eq. (1).

$$HV_{norm,i}(t_{AA}) = \frac{\Delta HV_i(\Delta t_{AA})}{\Delta HV_{i,max}} = \frac{HV_i(t_{AA}) - HV_i(t_0)}{\Delta HV_{i,max}}. \quad (1)$$

This relative hardness parameter was now related directly to change in volume fraction of precipitates (Eq. 2). Furthermore, it was assumed, that the volume fraction reached a maximum at the time of peak hardness, represented by ageing time  $t_{PA}$ .

$$HV_{norm,i}(t_{AA}) = \frac{f(t_{AA})}{f_{max}} = \frac{f(t_{AA})}{f(t_{PA})}. \quad (2)$$

The evolution of precipitate volume fraction can be mathematically described via the Avrami-equation [9],

$$\frac{f(t_{AA})}{f_{max}} = 1 - \exp\left(-\left(\frac{t_{AA}}{\tau}\right)^q\right), \quad (3)$$

where  $q$  is a time exponent which is linked to the nucleation and growth rate, and  $\tau$  represents a characteristic time [10]. Values for  $\tau$  were taken from the normalized hardness evolution via extrapolation, but since values for  $q$  were fitted, it was assumed that the nucleation characteristics stayed constant over the ageing period.

With respect to the particle type the following assumptions were made: They were considered to be of  $\beta''$ -type ( $Mg_5Si_6$ ); cell structure, chemistry and a rod shape with a cross section of 4 nm by 4 nm were defined according to [11]. Furthermore, the precipitates were assumed to be spherical and to have the same hardening effect as rod-shaped particles with identical volumes, i.e. an equivalent radius can be calculated. Precipitates were taken to be monodisperse, and since only one type of particle was accounted for, only one effective interfacial energy of  $\beta''$  and the matrix existed, with  $\gamma = 0.238$  J/m<sup>2</sup>. This value was found by 3IVM+ parameter tuning runs described in [5] and is in good agreement with values found in literature [1]. A further assumption was that at peak age condition the maximum possible volume fraction of  $\beta''$  particles was reached for each alloy, taking into account the matrix solubility of Mg and Si in Al at 180 °C, i.e.  $2.0 \cdot 10^{-4}$  at-% for Mg and  $3.0 \cdot 10^{-4}$  at-% for Si, respectively [12]. Thus, the the largest possible volume fraction of precipitates  $f_{\beta'',max}$  can be calculated from Eq. (4):

$$f_{\beta'',max} = \left(c_i^{0a} - c_{i,\alpha,180^\circ C}^a\right) \cdot \frac{1}{f_{i,\beta''}^a} \frac{n_\alpha V_{\beta'',uc}}{n_{\beta''} a_{\alpha,uc}^3}. \quad (4)$$

Here  $i$  stands for the element constraining  $f_{\beta'',max}$ ,  $c_i^{0a}$  is the atomic concentration of element  $i$ ,  $c_{i,\alpha,180^\circ C}^a$  the matrix solubility of element  $i$  at 180 °C,  $f_{i,\beta''}^a$  the atomic fraction of  $i$  in  $\beta''$  (i.e. 5/11 for  $i = Mg$  and 6/11 for  $i = Si$ ),  $n_\alpha$  the number of atoms in a matrix unit cell,  $n_{\beta''}$  the number of atoms in the  $\beta''$ -supercell (i.e.  $n_{\beta''} = 22$ ) [11], and  $a_{\alpha,uc}$  the lattice parameter of Al,  $4.05 \cdot 10^{-10}$  m [12].

Concentrations of Mg and Si in solid solution at ageing time  $t_{AA}$ , i.e.  $c_{ss,Mg}(t_{AA})$  and  $c_{ss,Si}(t_{AA})$ , respectively, can be calculated as

$$c_{j,ss}^a(t_{AA}) = c_j^{0a} - f_{\beta^*}(t_{AA})Z \cdot \frac{a_{\alpha,uc}^3}{V_{\beta^*,uc}^n}, \quad (5)$$

where the index  $j$  stands for either Mg or Si and  $Z = 2.5$  if  $j = \text{Mg}$  and  $Z = 3$  if  $j = \text{Si}$ . The evolution of the mean radius with ageing time was calculated according to Eq. (6) [13],

$$r(t_{AA})^3 - r(t_0)^3 = k \cdot t_{AA}, \quad (6)$$

with the fitted value  $k = 2 \cdot 10^{-22} \text{ m}^3/\text{h}$ , and  $r(t_0)$  was set to  $1 \cdot 10^{-9} \text{ m}$  [3].

NaMo has a built-in particle size distribution (PSD) model that simulates the precipitate size distributions for a wide range of alloys during arbitrary heat treatment routes, i.e. also non-isothermal heat treatments are possible [4]. NaMo simulations of the 180 °C ageing treatment were conducted for materials 1 and 2. It has to be noted that no calibration of model parameters to the used alloys was executed.

#### 4. Results

Fig. 1 shows the evolution of Vickers Hardness HV and yield stress  $\sigma_y$  for all materials during artificial ageing at 180 °C. Here, good agreement of HV and  $\sigma_y$  values was observed, although HV measurements showed slightly faster kinetics for material 2 and material P. Material 1 differed strongly from the other three alloys, having the slowest kinetics. Material 2 reached the highest yield stress with 270 Mpa. Ageing times to peak age condition according to hardness measurements were  $\sim 17 \text{ h}$  for material 1 and  $\sim 2 \text{ h}$  for alloys 2, 3 and P. The fitted curves and results for  $\tau$  and  $q$  of all materials are shown in Fig. 2; fitting was done via the least square method.

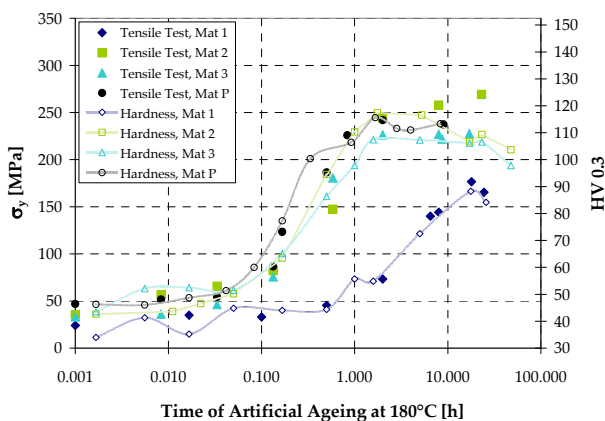


Fig. 1: Vickers Hardness (HV 0.3) and yield stress after various ageing times  $t_{AA}$

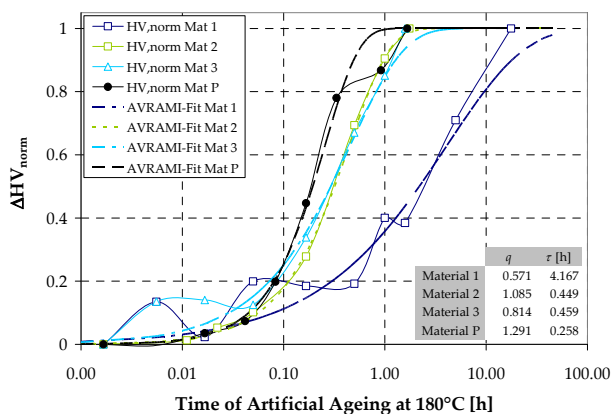


Fig. 2: Avrami-fits for all alloys

Table 2 shows the outcome of volume fractions and mean radius modeling of precipitates  $\beta''$  for 3IVM+ input at peak age condition and simulation results from NaMo and experimental findings via TEM observations, which were performed on materials 1 and 2 at peak age [14]. The TEM results proved that the particles at peak-age condition were of  $\beta''$ -type and appeared at a high number density ( $> 2 \cdot 10^{22} \text{ m}^{-3}$ ) [14]. For materials 1 and 2 Mg was the element limiting the maximum  $\beta''$  volume fraction, for the other two alloys it was Si [5]. Both microchemistry inputs for 3IVM+ and NaMo's particle size distribution model results showed good agreement with TEM data, especially for material 1. For material 2 the  $\beta''$  volume fraction of 0.0243 found by TEM was higher than predicted by calculations with the assumptions and data of [11], i.e. a maximum  $\beta''$  volume fraction of 0.0151.

With the made assumptions it was possible to model the yield stress values over ageing by 3IVM+. The results are shown in Fig. 3, and compared to the predictions of NaMo and experimentally measured yield stress values. For 3IVM+ good agreement of the yield stress with experiments was found for solution heat treated, near peak age, and peak aged conditions for all alloys, with a deviation of < 20 MPa at these stages. In the underaged condition the yield stress was overpredicted for all alloys. For material 2 this difference amounted up to 75 MPa.

Table 2: Volume fractions  $f$  and mean precipitate radii  $r_{\beta'',PA}$  at peak age condition [14].

	3IVM+		NaMo – Psd model		TEM Data	
	$f_{\beta'',PA}$ (1)	$r_{\beta'',PA}$ (nm)	$f_{\beta'',PA}$ (1)	$r_{\beta'',PA}$ (nm)	$f_{\beta'',PA}$ (1)	$r_{eq,\beta'',PA}$ (nm)
Material 1	0.0068	5.06	0.0058	5.02	0.0089	5.12
Material 2	0.0150	2.67	0.0092	4.75	0.0243	3.57
Material 3	0.0104	2.67	-	-	-	-
Material P	0.0117	2.62	-	-	-	-

Fig. 3 b) shows the results of a direct comparison of 3IVM+ and NaMo, which was done by simulating the yield stress via 3IVM+ with microchemistry input calculated by NaMo's integrated PSD-model. These simulations were conducted for Materials 1 and 2. Here 3IVM+ led to low yield stress values for material 2 for ageing times greater than 1h and too high yield stresses from underaged to close to peak age condition for material 1.

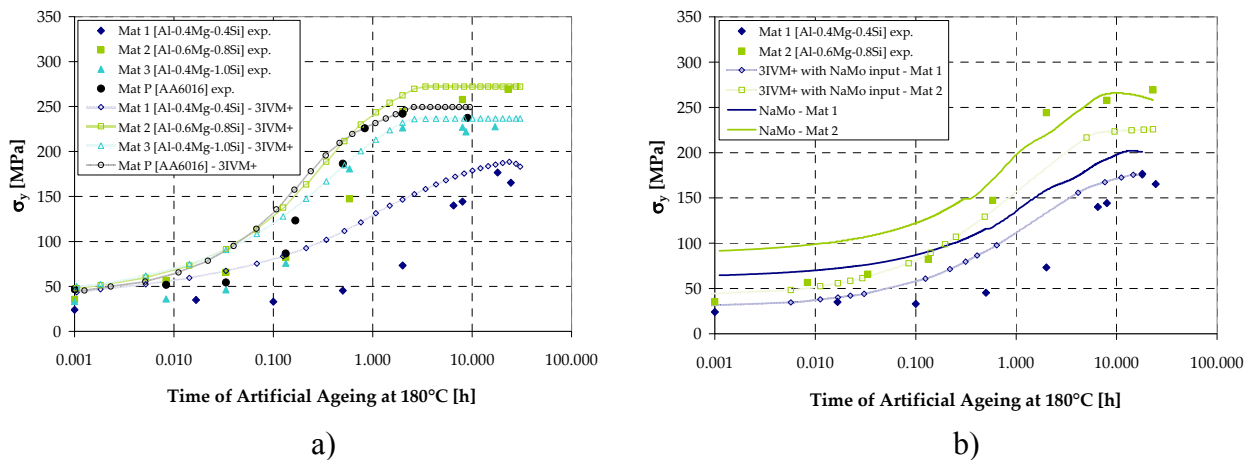


Fig. 3: Strength modeling compared to experimental results, a) 3IVM+, b) NaMo and 3IVM+ with NaMo microchemistry input.

## 5. Discussion

Material 1 showed the slowest kinetics in HV and tensile testing results. This was presumably due to the low Mg concentration in combination with a low Si amount, limiting fast and successful precipitate formation through diffusion. Faster ageing of material 2 and P was attributed to their high effective Mg content. Comparing material 3 and P, which have nearly the same amount of Mg and Si, the effect of the additional alloying elements of material P led to faster kinetics and higher strength.

Good correspondence of measured and predicted volume fractions and mean radii of precipitates at peak age was found. For underaged conditions the assumptions of only  $\beta''$  particles being present and the precipitate volume fraction being directly linked to the hardness increase, led to a too fast strength increase for nearly all alloys. This discrepancy presumably resulted from neglecting early metastable phases such as atom clusters or GP-I zones within the microchemistry model, which

develop prior to  $\beta''$  in the precipitation sequence of Al-Mg-Si [11], and because of their small size and better coherency with the matrix generate less hardening from particle-dislocation interactions [10, 12].

## 6. Summary

For four different AA6xxx materials, three high purity Al-Mg-Si and one commercial AA6016 alloy, the yield stress evolution during artificial ageing at 180 °C was computed by 3IVM+, compared to the established age hardening model NaMo and to experimental findings from hardness testing, tensile testing and TEM data from two alloys at peak age condition. To provide the missing microchemistry input for 3IVM+ assumptions were made, mainly assuming only one type of particle, i.e.  $\beta''$ , and connecting the hardness evolution to the precipitated volume fraction. This approach worked well for solution heat treated, close to peak age, and peak aged condition. However, for early ageing stages the strength was overpredicted. To successfully model yield stresses or even complete flow curves during various ageing stages of AA6xxx with 3IVM+, the flow stress model has to be linked with more advanced microchemistry models that reflect the complex precipitation sequences including metastable phases in this type of alloys.

## 7. Acknowledgements

The author likes to thank Hydro Aluminium Deutschland for providing the material and Z. Liang from Helmholtz-Zentrum Berlin for TEM measurements.

## References

- [1] O. R. Myhr, Ø. Grong, H. G. Fjær, and C. D. Marioara: *Acta Materialia* 52 (2004) 4997-5008.
- [2] M. Crumbach, M. Goerdeler, G. Gottstein, H. Aretz, and R. Kopp: *Modelling and Simulation in Materials Sc. and Eng.* 14 (2006) 835-856.
- [3] S. Esmaeili, D. J. Lloyd, and W. J. Poole: *Acta Materialia* 51 (2003) 2243-2257.
- [4] Ø. Grong and O. R. Myhr, 2007: *Combined precipitation, yield strength and work hardening models for Al-Mg-Si alloys*, (9th Intl. Summer School on Aluminum Alloy Technology, Trondheim, Norway, 2007).
- [5] T. Brüggemann: *Investigation and simulation of the age-hardening-behaviour of AA6xxx alloys for car-body applications after different pre-treatments*, diploma thesis, (IMM, RWTH Aachen, 2009).
- [6] M. Goerdeler: *Application of a Dislocation Density Based Flow Stress Model in the Integrative Through Process Modelling of Aluminium Production*, doctoral dissertation, (Shaker, Aachen, 2007).
- [7] V. Mohles, X. Li, C. Heering, G. Hirt, S. Bauhmik, and G. Gottstein: *An improved dislocation density based flow stress model for Al-alloys: 3IVM+*, Conf. Proc., (ESAFORM2008, Lyon, 2008).
- [8] F. Roters: *Realisierung eines Mehrebenenkonzeptes in der Plastizitätsmodellierung*, doctoral dissertation, (Shaker, Aachen, 1999).
- [9] D. H. Bratland, R. Grong, H. Shercliff, O. R. Myhr, and S. Tjørrta: *Acta Materialia* 45 (1997) 1-22.
- [10] G. Gottstein: *Physical Foundations of Materials Science*, (Springer-Verlag, Berlin, 2004).
- [11] C. D. Marioara: *A TEM study of the precipitates in a 6082 Al-Mg-Si alloy system*, doctoral dissertation, (Faculty of Natural Sciences and Technology, NTNU Trondheim, 2000).
- [12] C. Kammer and A. Z. Düsseldorf: *Aluminium-Taschenbuch. 1. Grundlagen und Werkstoffe*, 14. Aufl., (Aluminium-Verl., Düsseldorf, 1995).
- [13] L. Löchte: *Real-Zeit skalierte Modellierung der Bildung und des Wachstums von Guinier-Preston-Zonen in AlCu-Legierungen*, doctoral dissertation, (Shaker, Aachen, 2000).
- [14] Z. Liang: *Investigation on the precipitation of Al-Mg-Si alloys with different heat treatments*, (Report of Helmholtz-Zentrum Berlin, 2008).